Neural Comput & Applic (2014) 25:1771–1783
DOI 10.1007/s00521-014-1668-z

ORIGINAL ARTICLE

# Coordinated formation pattern control of multiple marine surface vehicles with model uncertainty and time-varying ocean currents

**Zhouhua Peng · Dan Wang · Hao Wang · Wei Wang**

Received: 29 October 2013 / Accepted: 5 July 2014 / Published online: 24 July 2014


**Abstract** This paper considers the coordinated formation pattern control of multiple marine surface vehicles in the presence of model uncertainty and time-varying ocean disturbances induced wind, waves and ocean currents. Leaderless and leader-follower formation controllers depending on the information of neighboring vehicles are devised based on a backstepping technique. Neural networks together with adaptive filtering methods are employed to extract the low frequency content of the model uncertainty and ocean disturbances. The results are further extended to the formation pattern control with unmatched time-varying ocean currents. An observer is developed to precisely identify the time-varying ocean currents. Then, observer-based leaderless and leader-follower formation controllers are proposed. For both cases, the stability properties of the multi-vehicle systems are established via Lyapunov analysis, and the formation tracking errors converge to an adjustable neighborhood of origin. An advantage of this design is that it results in adaptive formation controllers with guaranteed low frequency control signals, which facilitates practical implementations. An example is given to show the performance of the proposed methods.

**Keywords** Distributed control · Formation control · Neural networks · Marine surface vehicles · Time-varying ocean current

Z. Peng (✉) · D. Wang · H. Wang · W. Wang
School of Marine Engineering, Dalian Maritime University, Dalian 116026, People's Republic of China
e-mail: zhouhuapeng@gmail.com

## 1 Introduction

In recent years, cooperative control of multiple vehicles has drawn significant attention [1, 2]. Applications of multi-vehicle systems can be found everywhere; in space, in the air, on land and at sea. Examples include formation flight of satellites, coordinated control of aerial vehicles, formation control of mobile robots and cooperative control of marine vehicles. Obviously, multi-vehicle systems enable individuals to collaborate with each other to perform difficult tasks, providing enhanced effectiveness and efficiency than a single one.

During the past decade, there has been considerable attention drawn to formation control of multiple marine surface vehicles (MSVs). Various approaches have been proposed, ranging from virtual structure framework [3], behavioral approach [4], leader-follower mechanisms [5–7], to synchronized path following framework [8]. Apparently, these control strategies only result in low-level cooperative behaviors. However, to execute more challenging missions, it requires the use of multiple vehicles working together to achieve a collective objective [1, 2, 9–11]. For example, a group of MSVs is required to achieve coverage in a sensor network, where the coverage center can be only known by a portion of vehicles for security reasons. They exchange their knowledge by communicating with a subset of nearby vehicles, in order to achieve the coverage. Obviously, such motion control scenario cannot be completed by those formation control strategies mentioned above.

A major constraint in a networked system is that the information flow can be severely restricted either for security reasons or for limited communication range. This situation is getting worse when a large lumber of vehicles are involved in the network. Consequently, centralized

controllers based on the information gathered by all agents are generally impractically to implement. Therefore, distributed control strategies based on neighborhood information have been widely explored in the literature [10–24]. These results are elegant. However, note that the agents are usually modeled as first-order systems [10–13], second-order systems [14–17], high-order systems [18] and general linear systems [19–23], which may not be adequate to describe the practical dynamics of MSVs as they undergo maneuvers in hazardous sea environment. Hopefully, the results shed some light onto the formation control of multiple MSVs discussed in this paper.

MSV possesses a lot of uncertainty in its dynamics such as payload variations, unmodeled hydrodynamics and time-varying ocean disturbances induced by wind, waves and ocean currents [25]. To deal with this problem, adaptive control methods have been suggested [26–32]. In [26], a projection-based adaptive controller is developed for ship with parametric uncertainty and unknown ocean disturbances. In [27], adaptive update laws are devised to estimate the unknown model parameters and bounded disturbances. In [26, 27], the uncertainty is assumed to be parametric. By designing the neural adaptive controllers, references [28–32] investigated the control problem of surface vehicles with unmodeled dynamics and ocean disturbances. It is well known that the ocean disturbances including wind, waves and ocean currents not only contain low frequency content, but also high frequency content. In particular, the adaptive methods given in [26–32] try to learn the vehicle uncertainty at arbitrary accuracy. However, from a practical perspective, only low frequency content can be compensated since the high frequency content is surely outside the bandwidth of actuators [33]. Therefore, it is of practical importance to derive an adaptive controller capable of extracting the low frequency content of ocean uncertainty.

Motivated by the above observations, this paper considers the coordinated formation pattern control of networked MSVs subject to dynamical uncertainty and ocean disturbances induced by wind, waves and ocean currents. In the leaderless case, the objective is to drive a group of MSVs to shape a relative formation pattern via local interactions. As for the leader-follower case, the objective is to force a group of MSVs to maintain a relative formation pattern with respect to a target point. Especially, only a subset of follower vehicles has access to the reference point. Neural networks, adaptive filtering and backstepping techniques are used to devise the formation controllers. Lyapunov analysis demonstrates that all signals in the closed-loop systems are uniformly ultimately bounded, and the formation tracking errors can be reduced as desired. An extension to the unmatched time-varying ocean currents is further studied. An observer is developed to identify the time-varying ocean currents at the kinematic level. An example is provided to show the performance of the proposed schemes. The main advantages are twofolds. First, the proposed scheme results in adaptive formation pattern controllers with guaranteed low frequency control signals, which facilitate practical implementations. Second, the time-varying ocean currents can be identified accurately and a relative formation pattern can be reached under the time-varying ocean currents.

In this paper, a practical design method, by combining neural networks, adaptive filtering and backstepping techniques, is proposed for formation pattern control of MSVs under hazardous sea environment. The comparisons with the exiting results are listed as below. In contrast to the formation controllers proposed in [3–8], the developed controllers hold a distributed nature in the sense that only neighboring information is used for feedback design. Compared with the adaptive controllers for marine vehicles in [26–32], the proposed adaptive controllers are able to capture the low frequency content of vehicle uncertainty and ocean disturbances. Finally, it is worth mentioning that the ocean currents at the vehicle kinematics are assumed to be constant in [34, 35], while this paper is the first trial to deal with the time-varying ocean currents.

This paper is organized as follows. Section 2 introduces some preliminaries and formulates the control problem. The leaderless and leader-follower formation controller designs are given in Sect. 3, both with rigorous stability analysis. The results are further extended to the formation pattern control in the presence of time-varying ocean currents in Sect. 4. Section 5 gives an example for illustrating the theoretical results. Section 6 concludes this paper.

*Notations* $||\cdot||$, $||\cdot||_F$ and $\mathrm{tr}(\cdot)$ denote the Euclidean norm, Frobenius norm and trace of a matrix, respectively. $\lambda_{\min}(\cdot)$, $\lambda_{\max}(\cdot)$ denote the smallest and biggest eigenvalue of a square matrix, respectively. The Kronecker product is denoted by $\otimes$. $I_N$ is an identity matrix of dimension $N$. $\mathrm{diag}\{A_1,\ldots,A_N\}$ denotes a block-diagonal matrix with the elements $A_i, i = 1,\ldots,N$, on its diagonal; here, $A_i$ can be a scalar or a matrix.

## 2 Preliminaries and problem formulation

### 2.1 Preliminaries

#### 2.1.1 Graph theory

Consider a system consisting of $N$ vehicles and a leader. Each vehicle is assumed to know its own state and has access to the state information from a subset of the vehicle group called the neighbor set denoted by $\mathcal{N}_i \subseteq \{1,\ldots,N\} \setminus \{i\}$. If each

vehicle is considered as a node, the neighbor relation can be described by a graph $\mathcal{G} = \{\mathcal{V}, \mathcal{E}\}$, where $\mathcal{V} = \{n_1, \ldots, n_N\}$ is a node set and $\mathcal{E} = \{(n_i, n_j) \in \mathcal{V} \times \mathcal{V}\}$ is an edge set with the element $(n_i, n_j)$ that describes the communication from node $i$ to node $j$. Further, define the adjacency matrix $\mathcal{A} = [a_{ij}] \in \mathbb{R}^{N\times N}$ with the diagonal entries $a_{ii} = 0$, and the non-diagonal entries $a_{ij} = 1$, if $(n_j, n_i) \in \mathcal{E}$; $a_{ij} = 0$, otherwise. Define the Laplacian matrix $L = [l_{ij}]$ with $l_{ij} = -a_{ij}$, if $j \neq i$, and $l_{ij} = \sum_{k=1}^{N} a_{ik}$, otherwise. If $a_{ij} = a_{ji}\ \forall i, j$; then, the graph $\mathcal{G}$ is undirected. If there is a path between any two nodes of an undirected network, then the graph $\mathcal{G}$ is connected. Finally, define a diagonal matrix $B = \text{diag}\{b_1, \ldots, b_N\}$ to be a leader adjacency matrix, where $b_i > 0$ if and only if the $i$th vehicle is a neighbor of the leader; otherwise, $b_i = 0$. For convenience, let $H = L + B$. The following lemmas play an important role in design and analysis of the proposed formation controllers.

**Lemma 1** [10] Let the graph $\mathcal{G}$ be undirected and connected, and at least, one vehicle has access to the leader. Then, the matrix $H$ is positive definite.

**Lemma 2** Let the graph $\mathcal{G}$ be undirected and connected; then, there exist a positive definite matrix $P$ such that $z^T L z = s^T P s$, where $z = [z_1, \ldots, z_N]^{\mathrm{T}}, s = [s_1, \ldots, s_N]^{\mathrm{T}}$, $s_i = \sum_{j=1}^{N} a_{ij}(z_i - z_j)$.

*Proof* The proof details can be found in [12], and thus, omitted here for brief.

**Lemma 3** [37] Let the graph $\mathcal{G}$ be undirected and connected. Then, $\lambda_2(L)\|x - \mathbf{1} \otimes \text{Ave}(x)\| \leq x^T L x$ where $\lambda_2(L)$ denotes the smallest nonzero eigenvalue of $L$, $x = [x_1, \ldots, x_N]^{\mathrm{T}} \in \mathbb{R}^n$ and $\text{Ave}(x) = \sum_{i=1}^{N} x_i$.

#### 2.1.2 Projection operator

**Definition 1** [38] Assume that an unknown $\theta^* \in \mathbb{R}^n$ exists $\|\theta^*\| \leq \theta_M^*$ with $\theta_M^* > 0$ and let $\theta$ be denoted by its estimation. Then, the projection operator $\text{Proj} : \mathbb{R}^n \to \mathbb{R}^n$ is defined as

$$\text{Proj}(y) \triangleq \begin{cases} y - \dfrac{\phi'(\theta)\phi'^T(\theta)y}{\|\phi'(\theta)\|^2}\phi(\theta), & \text{if } \phi(\theta) \geq 0 \text{ and } \phi'(\theta)y < 0, \\ y, & \text{otherwise,} \end{cases} \tag{1}$$

where $\phi : \mathbb{R}^n \to \mathbb{R}$ is a continuously differentiable convex function

$$\phi(\theta) = \frac{\theta^{\mathrm{T}}\theta - \vartheta^2}{2\varepsilon_\theta \vartheta + \varepsilon_\theta^2}, \tag{2}$$

where $\vartheta$ and $\varepsilon_\theta$ are positive constants with $\vartheta = \theta_M^*$. $\phi'(\theta) = \partial\phi/\partial\theta$.

Given $\theta(0) \leq \vartheta$, the projection operator takes the following properties

$$\begin{aligned} &\|\theta(t)\| \leq \theta_M, \forall\, t \geq 0, \\ &\|\tilde{\theta}\| \leq \tilde{\theta}_M, \forall\, t \geq 0, \\ &\tilde{\theta}^{\mathrm{T}}[\text{Proj}(y) - y] \leq 0, \end{aligned} \tag{3}$$

where $\tilde{\theta} = \theta - \theta^*$, $\theta_M = \vartheta + \varepsilon_\theta$, $\tilde{\theta}_M = 2\vartheta + \varepsilon_\theta$,

Moreover, the definition of the projection operator can be generalized to matrices as $\text{Proj}(Y)$, where $\Theta \in \mathbb{R}^{n\times m}$ and $Y \in \mathbb{R}^{n\times m}$. In this case, it follows from the property (3) that

$$\text{tr}[(\Theta - \Theta^*)^{\mathrm{T}}(\text{Proj}(Y) - Y)] \leq 0, \Theta^* \in \mathbb{R}^{n\times m}, \tag{4}$$

where $\Theta^*$ denotes the true value of $\Theta$.

### 2.2 Problem formulation

#### 2.2.1 Vehicle model

To describe the motion of MSV, two reference frames are used, a local earth-fixed frame and a body-fixed frame, as depicted in Fig. 1. The components $\eta_i = [x_i, y_i, \psi_i]$ are the northeast positions $(x_i, y_i)$ of the vehicle relative to the earth-fixed frame and the yaw angle $\psi_i$ relative to the north. The components of the velocity vector $v_{ir} = [u_{ir}, v_{ir}, r_i]^{\mathrm{T}}$ are the surge and sway velocities relative to ocean currents $(u_{ir}, v_{ir})$ and the yaw rate $r_i$. Here, the fluid is assumed to be irrotational. Consider a group of $N$ MSVs governed by the following model [25] with kinematics

$$\dot{\eta}_i = R(\psi_i)v_{ir} + V_{ic}(t), \tag{5}$$

and kinetics

$$M_i\dot{v}_{ir} + C_i(v_{ir})v_{ir} + D_i(v_{ir})v_{ir} + g_i(\eta_i, v_{ir}) = \tau_i + \tau_{ien}(t), \tag{6}$$

where

$$R(\psi_i) = \begin{bmatrix} \cos\psi_i & -\sin\psi_i & 0 \\ \sin\psi_i & \cos\psi_i & 0 \\ 0 & 0 & 1 \end{bmatrix}; \tag{7}$$

where $M_i = M_i^T \in \mathbb{R}^{3\times3}, C_i(v_{ir}) \in \mathbb{R}^{3\times3}, D_i(v_{ir}) \in \mathbb{R}^{3\times3}$ denote the inertia matrix, coriolis/centripetal matrix and damping matrix, respectively; $g_i(\eta_i, v_{ir}) = [g_{iu}, g_{iv}, g_{ir}]^{\mathrm{T}} \in \mathbb{R}^3$ is unknown term including the restoring forces due to gravity and buoyancy forces, and other unmodeled dynamics; $\tau_i = [\tau_{iu}, \tau_{iv}, \tau_{ir}]^{\mathrm{T}} \in \mathbb{R}^3$ denotes the control input; $\tau_{ien}(t) = [\tau_{ienu}(t), \tau_{ienv}(t), \tau_{ienr}(t)]^{\mathrm{T}} \in \mathbb{R}^3$ is the resulting environmental force and moment vector due to wind and waves. $V_{ic}(t) = [\upsilon_{ix}(t), \upsilon_{iy}(t), 0]^{\mathrm{T}} \in \mathbb{R}^3$ is the vector representing the time-varying ocean currents.

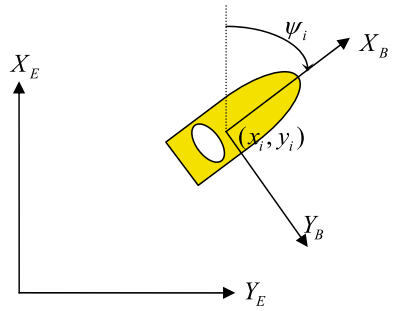


**Fig. 1** Reference frames: earth-fixed and body-fixed

*Remark 1* In the literature, a variety of motion control concepts has been proposed and validated on the vehicle model, e.g., dynamic positioning [30], trajectory tracking [28, 31], mooring control [29], path following [8, 36]. In fact, this model represents a large number of marine vehicles in practice. It is should be noted that most vehicles are underactuated at high speeds and are forced to maneuver in an energy-efficient manner. However, this paper aims to shape a relative stationary formation pattern at the sea surface. Therefore, low speed operations are enabled and the vehicles considered are fully actuated.

### 2.2.2 Control objective

**Definition 2** A desired geometric formation pattern is defined as $\mathcal{P} = \{\mathcal{P}_i\}$ where $\mathcal{P}_i = [p_{ix}, p_{iy}, p_{i\psi}]^{\mathrm{T}}$, $i = 1, \ldots, N$, and $p_{ix}, p_{iy}, p_{i\psi}$ are constants.

Without losing of generality, assume that $\sum_{i=1}^{N} \mathcal{P}_i = [0, 0, 0]^{\mathrm{T}}$, i.e., the center of the geometric pattern $\mathcal{P}$ is at the origin of the earth-fixed frame.

*Remark 2* For simplicity, a static relative formation pattern is considered here, i.e., $\dot{\mathcal{P}}_i = 0$.

Define $\mathcal{P}_{ij} = \mathcal{P}_i - \mathcal{P}_j$. Then, the *control objective* is to design a distributed control law $u_i$ to achieve the geometric formation pattern $\mathcal{P}$, i.e.,

$$\lim_{t\to\infty} \|\eta_i - \eta_j - \mathcal{P}_{ij}\| \le \delta_1,\ i \ne j, \tag{8}$$

where $\delta_1$ is a positive constant which can be made sufficiently small.

In many instances, it is desirable that the formation pattern center of MSVs arrives at a given reference point $\eta_r \in \mathbb{R}^3$. Then, the leader-follower formation pattern control is to achieve the formation pattern $\mathcal{P}$ with a desired reference point $\eta_r$, i.e.,

$$\lim_{t\to\infty} \|\eta_i - \eta_j - \mathcal{P}_{ij}\| \le \delta_2,\ i \ne j, \tag{9}$$

$$\lim_{t\to\infty} \left\| \sum_{i=1}^{N} \frac{\eta_i}{N} - \eta_r \right\| \le \delta_3, \tag{10}$$

where $\delta_2$ and $\delta_3$ are positive constants which can be made sufficiently small.

*Remark 3* Inequality (9) means that the MSVs converge to the formation pattern $\mathcal{P}$ with bounded errors. Inequality (10) indicates that the center of the formation pattern nearly converges to the desired reference point $\eta_r$.

The following assumptions are made in the following controller design.

**Assumption 1** The network $\mathcal{G}$ is undirected and connected.

**Assumption 2** [33] A nonlinear function $f_i(\chi_i, t)$ can be approximated by a neural network as

$$f_i(\chi_i, t) = W_i^T(t)\varphi_i(\chi_i) + \varepsilon_i(\chi_i),\ \forall \chi_i \in \mathcal{D}, \tag{11}$$

where $W_i(t)$ is an unknown time-varying matrix satisfying $\|W_i(t)\|_F \le W_{iM}$ and $\|\dot{W}_i\|_F \le W_{iM}^d$ with $W_{iM} \in \mathbb{R}, W_{iM}^d \in \mathbb{R}$ positive constants; $\varphi_i(\chi_i) : \mathcal{D} \to \mathbb{R}^s$ is a known vector function of the form $\varphi_i(\chi_i) = [\varphi_{i1}(\chi_i), \varphi_{i2}(\chi_i), \ldots, \varphi_{is}(\chi_i)]^{\mathrm{T}}$ satisfying $\|\varphi_i\| \le \varphi_{iM}$ with $\varphi_{iM}$ a positive constant, and $\mathcal{D}$ is a compact set; $\varepsilon_i(\chi_i)$ is the approximation error satisfying $\|\varepsilon_i(\chi_i)\| \le \varepsilon_{iM}$ with $\varepsilon_{iM}$ a positive constant.

*Remark 4* In assumption 2, the requirement of constant NN weight is relaxed by allowing for time-varying NN weight such that time-varying disturbances can be incorporated into the NN approximation.

## 3 Coordinated formation pattern control

In this section, we first consider the vehicle model with matched model uncertainty and matched ocean disturbances induced by wind and waves, i.e., $V_{ic}(t) \equiv 0$. The unmatched disturbance induced by ocean currents will be addressed in the Sect. 4.

### 3.1 Leaderless formation pattern control

In the following, we show that how to use the neural networks, adaptive filtering and backstepping [39] techniques to develop the distributed formation controller. The design procedure is elaborated as follows.

**Step 1.** Define two variables

$$\begin{cases} z_{i1} = \eta_i - \mathcal{P}_i, \\ z_{i2} = v_{ir} - \alpha_{i1}, \end{cases} \tag{12}$$

where $\alpha_{i1} \in \mathbb{R}^3$ is a virtual control input. Take the time derivative of $z_{i1}$, and it follows that

$$\dot{z}_{i1} = R_i\alpha_{i1} + R_i z_{i2}, \tag{13}$$

where $R_i = R(\psi_i)$.

Then, a distributed kinematic virtual control law $\alpha_{i1}$ based on the local information is proposed as follows

$$\alpha_{i1} = -K_{i1}R_i^T s_i, \tag{14}$$

where $K_{i1} = \mathrm{diag}\{k_{i11}, k_{i12}, k_{i13}\}$ is a diagonal matrix with $k_{i11} \in \mathbb{R}, k_{i12} \in \mathbb{R}, k_{i13} \in \mathbb{R}$ being positive constants; $s_i$ is defined as

$$s_i = \sum_{j\in\mathcal{N}_i} a_{ij}(\eta_i - \eta_j - \mathcal{P}_{ij}). \tag{15}$$

where $a_{ij}$ is defined in Sect. 2.1.1.

Substituting (14) into (13) yields

$$\dot{z}_{i1} = -K_{i1}s_i + R_i z_{i2}, \tag{16}$$

Let $z_1 = [z_{11}^T, \ldots, z_{N1}^T]^{\mathrm{T}}$, $z_2 = [z_{12}^T, \ldots, z_{N2}^T]^{\mathrm{T}}$, $s = [s_1^T, \ldots, s_N^T]^{\mathrm{T}}$, $\mathcal{R} = \mathrm{diag}\{R(\psi_1), \ldots, R(\psi_N)\}$, $K_1 = \mathrm{diag}\{K_{11}, \ldots, K_{N1}\}$. Then, the $N$ subsystem (13) with (16) can be expressed as

$$\dot{z}_1 = -K_1 s + \mathcal{R}z_2, \tag{17}$$

Consider a Lyapunov function candidate

$$\mathcal{V}_{11} = \frac{1}{2}z_1^T(L \otimes I_3)z_1, \tag{18}$$

whose time derivative along (17) is given by

$$\dot{\mathcal{V}}_{11} = -s^T K_1 s + s^T \mathcal{R} z_2. \tag{19}$$

**Step 2.** Taking the time derivative of $z_{i2}$ yields

$$\begin{aligned} M_i\dot{z}_{i2} = &-C_i(v_{ir})v_{ir} - D_i(v_{ir})v_{ir} - g_i(\eta_i, v_{ir}) + \tau_i \\ &+ \tau_{ien}(t) - M_i\dot{\alpha}_{i1}. \end{aligned} \tag{20}$$

Then, consider the second Lyapunov function candidate

$$\mathcal{V}_{12} = \mathcal{V}_{11} + \frac{1}{2}z_2^T M z_2, \tag{21}$$

where $M = \mathrm{diag}\{M_1, \ldots, M_N\}$. Its time derivative with (20) is

$$\begin{aligned} \dot{\mathcal{V}}_{12} = &-s^T K_1 s + \sum_{i=1}^{N}\{z_{i2}^T(-C_i(v_{ir})v_{ir} - D_i(v_{ir})v_{ir} \\ &- g_i(\eta_i, v_{ir}) + \tau_i + \tau_{ien}(t) - M_i\dot{\alpha}_{i1} + R_i^T s_i)\}. \end{aligned} \tag{22}$$

The desired kinetic control law $\tau_i$ is chosen as

$$\tau_i = -K_{i2}z_{i2} - R_i^T s_i + f_i(\chi_i, t), \tag{23}$$

where $f_i(\chi_i, t) = [f_i^u(\cdot), f_i^v(\cdot), f_i^r(\cdot)]^{\mathrm{T}} = M_i\dot{\alpha}_{i1} + C_i(v_{ir})v_{ir} + D_i(v_{ir})v_{ir} + g_i(\eta_i, v_{ir}) - \tau_{ien}(t)$ with $\chi_i = [1, \eta_i, \eta_j, v_{ir}, v_{jr}]^{\mathrm{T}}$, $j \in \mathcal{N}_i$ ; $f_i^u(\cdot), f_i^v(\cdot)$ and $f_i^r(\cdot)$ denote the uncertainty in surge, sway and yaw directions, respectively; $K_{i2} = \mathrm{diag}\{k_{i21}, k_{i22}, k_{i23}\} \in \mathbb{R}^{3\times 3}$ with $k_{i21} \in \mathbb{R}, k_{i22} \in \mathbb{R}, k_{i23} \in \mathbb{R}$ being positive constants.

Note that without the explicit knowledge of $C_i, D_i, g_i, M_i, \tau_{ien}(t)$, the controller given in (23) cannot be available. Then, let $f_i(\chi_i, t)$ be approximated by the NN in (11).

In what follows, a practical kinetic control law is constructed as follows

$$\tau_i = -K_{i2}z_{i2} - R_i^T s_i + \tau_{ia}, \tag{24}$$

where $\tau_{ia} = [\tau_{ia}^u, \tau_{ia}^v, \tau_{ia}^r]^{\mathrm{T}}$ is an adaptive term designed as

$$\tau_{ia} = \hat{W}_i^T(t)\varphi_i(\chi_i). \tag{25}$$

$\hat{W}_i(t)$ is an estimate of $W_i(t)$ that updated as

$$\dot{\hat{W}}_i(t) = \Gamma_{iW}\mathrm{Proj}\{-\varphi_i(\chi_i)z_{i2}^T + k_W[\hat{W}_{if}(t) - \hat{W}_i(t)]\}, \tag{26}$$

and $W_{if}(t)$ is a low-pass filter weight estimate of $W_i(t)$ given by

$$\dot{\hat{W}}_{if}(t) = \Gamma_{if}\mathrm{Proj}\{\hat{W}_i(t) - \hat{W}_{if}(t)\}, \tag{27}$$

where $k_W \in \mathbb{R}, \Gamma_{iW} \in \mathbb{R}, \Gamma_{if} \in \mathbb{R}$ are positive constants.

Substituting the control law (24) into (22) yields

$$\dot{\mathcal{V}}_{12} = -s^T K_1 s - z_2^T K_2 z_2 + \sum_{i=1}^{N} z_{i2}^T[\tilde{W}_i^T(t)\varphi_i(\chi_i) - \varepsilon_i], \tag{28}$$

where $K_2 = \mathrm{diag}\{K_{12}, \ldots, K_{N2}\}$ and $\tilde{W}_i(t) = \hat{W}_i(t) - W_i(t)$.

The first result of this paper is stated as follows.

**Theorem 1** Consider a networked system consisting of $N$ MSVs governed by the dynamics (5, 6) with Assumptions 1 and 2 satisfied. Select the control law (24) with the adaptive laws (26) and (27). Then, all the signals in the closed-loop system are uniformly ultimately bounded (UUB), and the formation pattern control errors $\eta_i - \eta_j - \mathcal{P}_{ij}$ satisfy (8) for some constant $\delta_1$ which can be adjusted to a small neighborhood of origin, provided that

$$\lambda_{\min}(K_2) > 1/2. \tag{29}$$

*Proof* Consider the augmented Lyapunov function candidate

$$\mathcal{V}_1 = \mathcal{V}_{12} + \frac{1}{2}\sum_{i=1}^{N}\left\{\mathrm{tr}\left(\tilde{W}_i^T\Gamma_{iW}^{-1}\tilde{W}_i\right) + k_W tr\left(\tilde{W}_{if}^T\Gamma_{if}^{-1}\tilde{W}_{if}\right)\right\}, \tag{30}$$

whose time derivative with (26, 27) and (28) is given by

$$\dot{\mathcal{V}}_1 = -s^T K_1 s - z_2^T K_2 z_2 + \sum_{i=1}^{N}\{-z_{i2}^T\varepsilon_i + \mathrm{tr}\{\tilde{W}_i^T[\varphi_i(\chi_i)z_{i2}^T + \Gamma_{iW}^{-1}\dot{\hat{W}}_i]\}\} + k_W tr\left(\tilde{W}_{if}^T\Gamma_{if}^{-1}\dot{\hat{W}}_{if}\right)\} - \mathrm{tr}\left[\left(\tilde{W}^T\Gamma_W^{-1} + k_W\tilde{W}_f^T\Gamma_f^{-1}\right)\dot{W}\right], \tag{31}$$

where $\tilde{W} = [\tilde{W}_1^T, \ldots, \tilde{W}_N^T]^{\mathrm{T}}$, $\dot{W} = [\dot{W}_1^T, \ldots, \dot{W}_N^T]^{\mathrm{T}}$, $\Gamma_W = \mathrm{diag}\{\Gamma_{1W}I_s, \ldots, \Gamma_{NW}I_s\}$, $\Gamma_f = \mathrm{diag}\{\Gamma_{1f}I_s, \ldots, \Gamma_{Nf}I_s\}$, $\tilde{W}_{if} = \hat{W}_{if} - W_i$.

After some manipulations, we have

$$\dot{\mathcal{V}}_1 \le -s^T K_1 s - z_2^T K_2 z_2 + \sum_{i=1}^{N}\{-z_{i2}^T\varepsilon_i + \mathrm{tr}\{\tilde{W}_i^T[\varphi_i(\chi_i)z_{i2}^T + k_W(\tilde{W}_i - \tilde{W}_{if}) + \Gamma_{iW}^{-1}\dot{\hat{W}}_i]\} + k_W tr\left[\tilde{W}_{if}^T(\tilde{W}_{if} - \tilde{W}_i + \Gamma_{if}^{-1}\dot{\hat{W}}_{if})\right]\} - \mathrm{tr}\left[\left(\tilde{W}^T\Gamma_W^{-1} + k_W\tilde{W}_f^T\Gamma_f^{-1}\right)\dot{W}\right]. \tag{32}$$

The property of the projection operator (4) leads to

$$\dot{\mathcal{V}}_1 \le -s^T K_1 s - z_2^T K_2 z_2 - z_2^T\varepsilon - \mathrm{tr}\left[\left(\tilde{W}^T\Gamma_W^{-1} + k_W\tilde{W}_f^T\Gamma_f^{-1}\right)\dot{W}\right], \tag{33}$$

where $\varepsilon = [\varepsilon_1^T, \ldots, \varepsilon_N^T]^{\mathrm{T}}$.

According to Assumption 2, $\varepsilon_i$, $W_i$ and $\dot{W}_i$ are bounded. Then, there exist positive constants $\varepsilon_M \in \mathbb{R}, W_M \in \mathbb{R}$ and $W_M^d \in \mathbb{R}$ such that $\|\varepsilon\| \le \varepsilon_M$, $\|W\|_F \le W_M$ and $\|\dot{W}\| \le W_M^d$. Using the projection properties in (3), we further obtain that there exist positive constants $\tilde{W}_M \in \mathbb{R}$ such that $\|\tilde{W}\|_F \le \tilde{W}_M$ and $\|\tilde{W}_f\|_F \le \tilde{W}_M$. Using Young's inequality yields

$$\begin{cases} |z_2^T\varepsilon| & \le \frac{1}{2}\|z_2\|^2 + \frac{1}{2}\varepsilon_M^2, \\ -\mathrm{tr}(\tilde{W}^T\Gamma_W^{-1}\dot{W}) & \le \lambda_{\max}(\Gamma_W^{-1})\tilde{W}_M W_M^d, \\ -\mathrm{tr}(\tilde{W}_f^T\Gamma_f^{-1}\dot{W}) & \le \lambda_{\max}(\Gamma_f^{-1})\tilde{W}_M W_M^d, \end{cases} \tag{34}$$

which leads to

$$\dot{\mathcal{V}}_1 \le -\lambda_{\min}(K_1)\|s\|^2 - [\lambda_{\min}(K_2) - 1/2]\|z_2\|^2 + \epsilon, \tag{35}$$

where

$$\epsilon = \frac{1}{2}\|\varepsilon_M\|^2 + [\lambda_{\max}(\Gamma_W^{-1}) + k_W\lambda_{\max}(\Gamma_f^{-1})]\tilde{W}_M W_M^d. \tag{36}$$

Note that either $\|s\| > \sqrt{\epsilon/\lambda_{\min}(K_1)}$, or $\|z_2\| > \sqrt{2\epsilon/[2\lambda_{\min}(K_2) - 1]}$, renders $\dot{\mathcal{V}}_1 < 0$. It follows that $s$ and $z_2$ are UUB [40]. Moreover, $\|s\|$ is bounded by $\|s\| \le \sqrt{\epsilon/\lambda_{\min}(K_1)}$.

By Lemmas 2 and 3, we further obtain

$$\frac{1}{2}\lambda_2(L)\|z_1 - \mathbf{1}\otimes\mathrm{Ave}(z)\|^2 \le s^T(P\otimes I_3)s, \tag{37}$$

which leads to

$$\|z_i - \mathrm{Ave}(z_1)\| \le \|z_1 - \mathbf{1}\otimes\mathrm{Ave}(z_1)\| \le \sqrt{\frac{2\lambda_{\max}(P)\epsilon}{\lambda_2(L)\lambda_{\min}(K_1)}}. \tag{38}$$

Note that

$$\|\eta_i - \eta_j - \mathcal{P}_{ij}\| \le \|z_{i1} - \mathrm{Ave}(z_1)\| + \|z_{j1} - \mathrm{Ave}(z_1)\|,$$

which directly implies (8) with $\delta_1$ taken as

$$\delta_1 = 2\sqrt{\frac{2\lambda_{\max}(P)\epsilon}{\lambda_2(L)\lambda_{\min}(K_1)}}. \tag{39}$$

Note that by increasing $K_{i1}$, the tracking bound $\delta_1$ can be adjusted very small. This completes the proof. □

### 3.2 Leader-follower formation pattern control

In the preceding section, the position center of the formation is generally not explicit. In practice, it is demandable for the group arrive at a reference point with a desired formation pattern. To deal with this case, a distributed leader-follower formation pattern controller is designed based on neural networks, adaptive filtering and backstepping.

**Step 1.** In this case, define

$$\begin{cases} q_{i1} = \eta_i - \mathcal{P}_i - \eta_r, \\ q_{i2} = v_{ir} - \alpha_{i2}. \end{cases} \tag{40}$$

Taking time derivative of $q_{i1}$ along (5) gives

$$\dot{q}_{i1} = R(\psi_i)\alpha_{i2} + R_i q_{i2}. \tag{41}$$

Since only a portion of vehicles has access to $\eta_r$, the traditional centralized position tracking control cannot be applied. Here, a distributed virtual control law $\alpha_{i2}$ based on the information of neighboring vehicles is proposed as follows

$$\alpha_{i2} = -K_{i1}R_i^T\zeta_i, \tag{42}$$

where $K_{i1}$ is defined the same as (14); $\zeta_i$ is defined as

$$\zeta_i = \sum_{j=1}^{N}[a_{ij}(\eta_i - \eta_j - \mathcal{P}_{ij}) + b_i q_{i1}], \tag{43}$$

where $b_i$ is defined in Sect. 2.1.1.

Substituting (42) into (41) yields

$$\dot{q}_{i1} = -K_{i1}\zeta_i + R_i q_{i2}. \tag{44}$$

Let $q_1 = [q_{11}^T, \ldots, q_{N1}^T]^{\mathrm{T}}$, $q_2 = [q_{12}^T, \ldots, q_{N2}^T]^{\mathrm{T}}$, $\zeta = [\zeta_{12}^T, \ldots, \zeta_{N2}^T]^{\mathrm{T}}$. Then, the $N$ subsystem of (44) resulting from $\zeta = (H \otimes I_3)q_1$ can be expressed by

$$\dot{q}_1 = -K_1(H \otimes I_3)q_1 + \mathcal{R}q_2. \tag{45}$$

**Step 2.** Taking the time derivative of $q_{i2}$, we have

$$\begin{aligned} M_i\dot{q}_{i2} = &- C_i(v_{ir})v_{ir} - D_i(v_{ir})v_{ir} - g_i(\eta_i, v_{ir}) + \tau_i \\ &+ \tau_{ien}(t) - M_i\dot{\alpha}_{i1}. \end{aligned} \tag{46}$$

Consider the following Lyapunov function candidate

$$\mathcal{V}_{21} = \frac{1}{2}q_1(H \otimes I_3)q_1 + \frac{1}{2}q_2^T M q_2, \tag{47}$$

whose time derivative along (45) and (46) satisfies

$$\begin{aligned} \mathcal{V}_{21} = &- \zeta^T K_1\zeta + \sum_{i=1}^{N}\Big\{q_{i2}^T(-C_i(v_{ir})v_{ir} - D_i(v_{ir})v_{ir} \\ &- g_i(\eta_i, v_{ir}) + \tau_i + \tau_{ien}(t) - M_i\dot{\alpha}_{i1} + R_i^T\zeta_i)\Big\}. \end{aligned} \tag{48}$$

Similar to the leaderless case, a practical kinetic controller is proposed as follows

$$\tau_i = -K_{i2}q_{i2} - R_i^T\zeta_i + \hat{W}_i^T(t)\varphi_i(\chi_i), \tag{49}$$

where $\hat{W}_i(t)$ is updated as

$$\dot{\hat{W}}_i(t) = \Gamma_{iW}\mathrm{Proj}\{-\varphi_i(\chi_i)q_{i2}^T + k_W[\hat{W}_{if}(t) - \hat{W}_i(t)]\}, \tag{50}$$

and $W_{if}(t)$ is updated as (27); $K_{i2}, \Gamma_{iW}, k_W$ are defined the same as in (26).

Substituting the control law (49) into (48) yields

$$\dot{\mathcal{V}}_{21} = -\zeta^T K_1\zeta - q_2^T K_2 q_2 + \sum_{i=1}^{N} q_{i2}^T[\tilde{W}_i^T(t)\varphi_i(\chi_i) - \varepsilon_i]. \tag{51}$$

Now, we are ready to state the second result of this paper.

**Theorem 2** Consider a networked system consisting of $N$ MSVs governed by the dynamics in (5) (6) with Assumptions 1–2 satisfied, and at least, one MSV has access to $\eta_r$. Select the control law (49) with the adaptive laws (50) and (27). Then, all the signals in the closed-loop system are UUB, and the formation pattern control errors $\eta_i - \eta_j - \mathcal{P}_{ij}$ satisfy (9) for some constant $\delta_2$ and the formation center arrives at $\eta_r$ with bounded errors $\delta_3$ given by (10), provided that

$$\lambda_{\min}(K_2) > 1/2. \tag{52}$$

*Proof* Consider the augmented Lyapunov function candidate

$$\mathcal{V}_2 = \mathcal{V}_{21} + \frac{1}{2}\sum_{i=1}^{N}\Big\{\mathrm{tr}(\tilde{W}_i^T\Gamma_{iW}^{-1}\tilde{W}_i) + \mathrm{tr}\Big(\tilde{W}_{if}^T\Gamma_{if}^{-1}\tilde{W}_{if}\Big)\Big\} \tag{53}$$

Using the adaptive laws (50, 27) and the property of the projection operator, one has

$$\begin{aligned} \dot{\mathcal{V}}_2 \le &- \zeta^T K_1\zeta - q_2^T K_2 q_2 - z_2^T\varepsilon - \mathrm{tr}\big[\big(\tilde{W}\Gamma_W^{-1} \\ &+ k_W\tilde{W}_f\Gamma_f^{-1}\big)\dot{W}\big], \end{aligned} \tag{54}$$

Using the inequality

$$|q_2^T\varepsilon| \le \frac{1}{2}\|q_2\|^2 + \frac{1}{2}\varepsilon_M^2, \tag{55}$$

it follows that

$$\dot{\mathcal{V}}_2 \le -\lambda_{\min}(K_1)\|\zeta\|^2 - [\lambda_{\min}(K_2) - 1/2]\|z_2\|^2 + \epsilon, \tag{56}$$

with $\epsilon$ defined in (36).

Note that either $\|\zeta\| > \sqrt{\epsilon/\lambda_{\min}(K_1)}$, or $\|q_2\| > \sqrt{2\epsilon/[2\lambda_{\min}(K_2) - 1]}$ makes $\dot{\mathcal{V}}_2 < 0$. It follows that $\zeta$ and $q_2$ are UUB. Furthermore, $\|\zeta\|$ is bounded by

$$\|\zeta\| \le \sqrt{\frac{\epsilon}{\lambda_{\min}(K_1)}}. \tag{57}$$

Noting that $\zeta = (H \otimes I_3)z_1$ and the fact $H$ is positive definite By Lemma 1, it follows that

$$\|q_{i1}\| \le \|q_1\| \le \sqrt{\frac{\epsilon}{\lambda_{\min}(H)\lambda_{\min}(K_1)}}, \tag{58}$$

implying (9) with $\delta_2$ taken as

$$\delta_2 = 2\sqrt{\frac{\epsilon}{\lambda_{\min}(H)\lambda_{\min}(K_1)}}.$$

Also, note that

$$\|\sum_{i=1}^{N}\frac{\eta_i}{N} - \eta_r\| \le \frac{\sum_{i=1}^{N}\|q_{i1}\|}{N}, \tag{59}$$

which leads to (9) with $\delta_3$ taken as

$$\delta_3 = \sqrt{\frac{\epsilon}{\lambda_{\min}(H)\lambda_{\min}(K_1)}}.$$

This completes the proof. □

*Remark 5* By choosing appropriate parameters $\Gamma_{if}$, the adaptive update laws (27) serve as low-pass filters. That is to say, $\hat{W}_{if}$ only contain the low frequency content of $\hat{W}_i$. In addition, the adaptive laws (26) try to minimize the difference between $\hat{W}_i$ and $\hat{W}_{if}$. As such, the low frequency control signals are guaranteed.

*Remark 6* Compared with adaptive control strategies for marine vehicles in [5, 7, 26–32], the proposed control

method takes the following advantage. In [26], a projection-based adaptive controller is developed to deal with the parametric model uncertainty and ocean disturbances. In [27], standard adaptive update laws are devised to estimate the unknown model parameters and ocean disturbances. In [5, 7, 28–32], neural adaptive controllers are developed to handle parametric model uncertainty, ocean disturbances and unmodeled dynamics. In all aforementioned results, the proposed controllers try to learn the uncertainty at arbitrary accuracy and did not provide any means for regulating the learning bandwidth of adaptive terms. However, the devised controllers are able to capture the low frequency content of the uncertainty and ocean disturbances, while preserve the stability of whole system, which results in practical implementable formation controllers.

## 4 Coordinated formation pattern control under time-varying ocean currents

This section addresses the formation pattern stability under the time-varying ocean currents.

### 4.1 Identification of time-varying ocean currents

In the following, an observer is developed to precisely identify the unknown time-varying ocean currents. The observer is designed at the kinematic level and has a simple structure. However, extra effort should be made to derive the stability of the entire system by putting together the observer and kinetic control law.

From (5), the position dynamics can be described by

$$\begin{cases} \dot{x}_i = u_i \cos(\psi_i) + v_i \sin(\psi_i) + \upsilon_{ix}(t), \\ \dot{y}_i = u_i \sin(\psi_i) + v_i \cos(\psi_i) + \upsilon_{iy}(t). \end{cases} \tag{60}$$

Let $\hat{\upsilon}_{ix}(t)$ and $\hat{\upsilon}_{iy}(t)$ be the estimate of $\upsilon_{ix}(t)$ and $\upsilon_{iy}(t)$, respectively, and then, a local observer is constructed as follows

$$\begin{cases} \dot{\hat{x}}_i = u_i \cos(\psi_i) + v_i \sin(\psi_i) + \hat{\upsilon}_{ix}(t) - \kappa_{i1}\tilde{x}_i, \\ \dot{\hat{y}}_i = u_i \sin(\psi_i) + v_i \cos(\psi_i) + \hat{\upsilon}_{iy}(t) - \kappa_{i2}\tilde{y}_i, \end{cases} \tag{61}$$

where $\tilde{x}_i = \hat{x}_i - x_i$ and $\tilde{y}_i = \hat{y}_i - y_i$ are observing errors; $\kappa_{i1} \in \mathbb{R}$ and $\kappa_{i2} \in \mathbb{R}$ are positive constants; $\hat{\upsilon}_{ix}(t)$ and $\hat{\upsilon}_{iy}(t)$ are updated as

$$\begin{cases} \dot{\hat{\upsilon}}_{ix}(t) = \Gamma_{ix}\mathrm{Proj}\{-\tilde{x}_i + k_x(\hat{\upsilon}_{ixf}(t) - \hat{\upsilon}_{ix}(t))\}, \\ \dot{\hat{\upsilon}}_{iy}(t) = \Gamma_{iy}\mathrm{Proj}\{-\tilde{y}_i + k_y(\hat{\upsilon}_{iyf}(t) - \hat{\upsilon}_{iy}(t))\}, \end{cases} \tag{62}$$

where $\hat{\upsilon}_{ixf}(t)$ and $\hat{\upsilon}_{iyf}(t)$ are low-pass filter weight estimates of $\hat{\upsilon}_{ix}(t)$ and $\hat{\upsilon}_{iy}(t)$ given by

$$\begin{cases} \dot{\hat{\upsilon}}_{ixf}(t) = \Gamma_{ixf}\mathrm{Proj}\{\hat{\upsilon}_{ix}(t) - \hat{\upsilon}_{ixf}(t)\}, \\ \dot{\hat{\upsilon}}_{iyf}(t) = \Gamma_{iyf}\mathrm{Proj}\{\hat{\upsilon}_{iy}(t) - \hat{\upsilon}_{iyf}(t)\}, \end{cases} \tag{63}$$

where $k_x \in \mathbb{R}, k_y \in \mathbb{R}, \Gamma_{ix} \in \mathbb{R}, \Gamma_{iy} \in \mathbb{R}, \Gamma_{ixf} \in \mathbb{R}, \Gamma_{iyf} \in \mathbb{R}]$ are positive constants. The resulting errors dynamics of $\tilde{x}_i$ and $\tilde{y}_i$ can be described by

$$\begin{cases} \dot{\tilde{x}}_i = -\kappa_{i1}\tilde{x}_i + \tilde{\upsilon}_{ix}, \\ \dot{\tilde{y}}_i = -\kappa_{i2}\tilde{y}_i + \tilde{\upsilon}_{iy}. \end{cases} \tag{64}$$

where $\tilde{\upsilon}_{ix} = \hat{\upsilon}_{ix} - \upsilon_{ix}$, and $\tilde{\upsilon}_{iy} = \hat{\upsilon}_{iy} - \upsilon_{iy}$.

The following lemma plays an important role in establishing the stability of the closed-loop system.

**Lemma 4** For kinematic dynamics (60) with the observer (61) and the adaptive laws (62, 63) guarantee that the error signals $\tilde{x}_i$, $\tilde{y}_i$, $\tilde{\upsilon}_{ix}$, $\tilde{\upsilon}_{iy}$ are UUB.

*Proof* Consider the following Lyapunov function candidate

$$\mathcal{V}_o = \sum_{i=1}^{N} \left\{ \tilde{x}_i^2 + \tilde{y}_i^2 + \Gamma_{ix}^{-1}\tilde{\upsilon}_{ix}^2 + \Gamma_{iy}^{-1}\tilde{\upsilon}_{iy}^2 + k_x\Gamma_{ixf}^{-1}\tilde{\upsilon}_{ixf}^2 + k_y\Gamma_{iyf}^{-1}\tilde{\upsilon}_{iyf}^2 \right\},$$

where $\tilde{\upsilon}_{ixf} = \hat{\upsilon}_{ixf} - \upsilon_{ix}$, and $\tilde{\upsilon}_{iyf} = \hat{\upsilon}_{iyf} - \upsilon_{iy}$. Its time derivative of which along (64) can be described by

$$\begin{aligned} \dot{\mathcal{V}}_o = \sum_{i=1}^{N} \Big\{ & -\kappa_{i1}\tilde{x}_i^2 - \kappa_{i2}\tilde{y}_i^2 + \tilde{\upsilon}_{ix}(\tilde{x}_i + \Gamma_{ix}^{-1}\dot{\hat{\upsilon}}_{ix}) + k_x\tilde{\upsilon}_{ixf}\Gamma_{ixf}^{-1}\dot{\hat{\upsilon}}_{ixf} \\ & + \tilde{\upsilon}_{iy}(\tilde{y}_i + \Gamma_{iy}^{-1}\dot{\hat{\upsilon}}_{iy}) + k_y\tilde{\upsilon}_{iyf}\Gamma_{iyf}^{-1}\dot{\hat{\upsilon}}_{iyf} - \tilde{\upsilon}_{ix}(\Gamma_{ix}^{-1} + k_x\Gamma_{ixf}^{-1})\upsilon_{ix} \\ & - \tilde{\upsilon}_{iy}(\Gamma_{iy}^{-1} + k_y\Gamma_{iyf}^{-1})\upsilon_{iy} \Big\}. \end{aligned} \tag{65}$$

Substituting the adaptive laws into (65) yields

$$\begin{aligned} \dot{\mathcal{V}}_o = \sum_{i=1}^{N} \Big\{ & -\kappa_{i1}\tilde{x}_i^2 - \kappa_{i2}\tilde{y}_i^2 - \tilde{\upsilon}_{ix}(\Gamma_{ix}^{-1} + k_x\Gamma_{ixf}^{-1})\dot{\upsilon}_{ix} \\ & - \tilde{\upsilon}_{iy}(\Gamma_{iy}^{-1} + k_y\Gamma_{iyf}^{-1})\dot{\upsilon}_{iy} \Big\}. \end{aligned} \tag{66}$$

Let $\kappa_1 = \mathrm{diag}\{\kappa_{11}, \ldots, \kappa_{N1}\}$, $\kappa_2 = \mathrm{diag}\{\kappa_{12}, \ldots, \kappa_{N2}\}$, $\Gamma_x = \mathrm{diag}\{\Gamma_{1x}, \ldots, \Gamma_{Nx}\}$, $\Gamma_y = \mathrm{diag}\{\Gamma_{1y}, \ldots, \Gamma_{Ny}\}$, $\Gamma_{xf} = \mathrm{diag}\{\Gamma_{1xf}, \ldots, \Gamma_{Nxf}\}$, $\Gamma_{yf} = \mathrm{diag}\{\Gamma_{1yf}, \ldots, \Gamma_{Nyf}\}$, $\tilde{x} = [\tilde{x}_1, \ldots, \tilde{x}_N]^{\mathrm{T}}$, $\tilde{y} = [\tilde{y}_1, \ldots, \tilde{y}_N]^{\mathrm{T}}$, $\tilde{\upsilon}_x = [\tilde{\upsilon}_{1x}, \ldots, \tilde{\upsilon}_{Nx}]^{\mathrm{T}}$, $\tilde{\upsilon}_y = [\tilde{\upsilon}_{1y}, \ldots, \tilde{\upsilon}_{Ny}]^{\mathrm{T}}$, and it follows that

$$\begin{aligned} \dot{\mathcal{V}}_o \le & -\tilde{x}^T\kappa_1\tilde{x} - \tilde{y}^T\kappa_2\tilde{y} - (\tilde{\upsilon}_x^T\Gamma_x^{-1} + k_x\tilde{\upsilon}_{fx}^T\Gamma_{xf}^{-1})\dot{\upsilon}_x \\ & - (\tilde{\upsilon}_y^T\Gamma_y^{-1} + k_y\tilde{\upsilon}_{fy}^T\Gamma_{yf}^{-1})\dot{\upsilon}_y. \end{aligned} \tag{67}$$

The projection operation leads to the following bound

$$\begin{aligned} & |-(\tilde{\upsilon}_x^T\Gamma_x^{-1} + k_x\tilde{\upsilon}_{fx}^T\Gamma_{xf}^{-1})\dot{\upsilon}_x| \le [\lambda_{\max}(\Gamma_x^{-1}) + k_x\lambda_{\max}(\Gamma_{xf}^{-1})]\tilde{\upsilon}_{xM}\upsilon_{xM}^d \\ & |-(\tilde{\upsilon}_y^T\Gamma_y^{-1} + k_y\tilde{\upsilon}_{fy}^T\Gamma_{yf}^{-1})\dot{\upsilon}_y| \le [\lambda_{\max}(\Gamma_y^{-1}) + k_y\lambda_{\max}(\Gamma_{yf}^{-1})]\tilde{\upsilon}_{yM}\upsilon_{yM}^d \end{aligned}$$

where $\tilde{\upsilon}_{xM} \in \mathbb{R}$, $\tilde{\upsilon}_{yM} \in \mathbb{R}$, $\upsilon_{xM}^d \in \mathbb{R}$, $\upsilon_{yM}^d \in \mathbb{R}$ are positive constants. Finally, one has

$$\dot{\mathcal{V}}_o \leq -\lambda_{\min}(\kappa_1)\tilde{x}^2 - \lambda_{\min}(\kappa_2)\tilde{y}^2 + \epsilon_o,$$

with $\epsilon_o = [\lambda_{\max}(\Gamma_x^{-1}) + k_x\lambda_{\max}(\Gamma_{xf}^{-1})]\tilde{\upsilon}_{xM}\upsilon_{xM}^d + [\lambda_{\max}(\Gamma_y^{-1}) + k_x\lambda_{\max}(\Gamma_{yf}^{-1})]\tilde{\upsilon}_{yM}\upsilon_{yM}^d$. Note that $\tilde{x} > \sqrt{\epsilon_o/\lambda_{\min}(\kappa_1)}$ and $\tilde{y} > \sqrt{\epsilon_o/\lambda_{\min}(\kappa_1)}$ renders $\dot{\mathcal{V}}_o < 0$. It follows that $\tilde{x}$ and $\tilde{y}$ are UUB. The projection operator ensures that the weights $\hat{\upsilon}_x$ and $\hat{\upsilon}_y$ are contained in compact sets for all $t$, which implies that $\tilde{\upsilon}_x$ and $\tilde{\upsilon}_y$ are UUB. The proof is complete. □

*Remark 7* The advantage of using an observer rather than using a direct adaptive control method to identify the ocean currents lies in the fact that it separates the estimate loop from the control loop, which enables an accurate and fast learning. This will be demonstrated in the simulation part.

*Remark 8* In [34], an observer is proposed to identify constant ocean currents. In [35], a direct adaptive method is employed to identify the constant ocean currents. This paper, to our best knowledge, is the first trial to deal with time-varying ocean currents.

### 4.2 Leaderless formation pattern control

In this case, taking the time derivative of $q_{i1}$, one has

$$\dot{z}_{i1} = R_i\alpha_{i1} + R_iz_{i2} + V_{ic}(t). \tag{68}$$

Then, a distributed kinematic control law $\alpha_{i1}$ based on the local information is proposed as follows

$$\alpha_{i1} = -K_{i1}R_i^T s_i - R_i^T\hat{V}_{ic}(t). \tag{69}$$

where $\hat{V}_{ic} = [\hat{\upsilon}_{ix}, \hat{\upsilon}_{iy}, 0]^{\mathrm{T}}$.

In essence, the left controller design follows the back-stepping technique, and thus, omitted here for brief. The kinetic controller is directly taken as (24).

In summary, the leaderless formation controller under time-varying ocean currents is constructed as follows.

Control laws:

$$\begin{cases} \tau_i = \hat{W}_i^T(t)\varphi_i(\chi_i) - K_{i2}z_{i2} - R_i^Ts_i, \\ \alpha_{i1} = -K_{i1}R_i^Ts_i - R_i^T\hat{V}_{ic}(t), \\ \dot{\hat{x}}_i = u_i\cos(\psi_i) + v_i\sin(\psi_i) + \hat{\upsilon}_{ix}(t) - \kappa_{i1}\tilde{x}_i, \\ \dot{\hat{y}}_i = u_i\sin(\psi_i) + v_i\cos(\psi_i) + \hat{\upsilon}_{iy}(t) - \kappa_{i2}\tilde{y}_i, \end{cases} \tag{70}$$

Adaptive laws:

$$\begin{cases} \dot{\hat{W}}_i(t) = \Gamma_{iW}\mathrm{Proj}\{-\varphi_i(\chi_i)z_{i2}^T + k_W[\hat{W}_{if}(t) - \hat{W}_i(t)]\}, \\ \dot{\hat{W}}_{if}(t) = \Gamma_{if}\mathrm{Proj}\{\hat{W}_i(t) - \hat{W}_{if}(t)\}, \\ \dot{\hat{\upsilon}}_{ix}(t) = \Gamma_{ix}\mathrm{Proj}\{-\tilde{x}_i + k_x(\hat{\upsilon}_{ixf}(t) - \hat{\upsilon}_{ix}(t))\}, \\ \dot{\hat{\upsilon}}_{iy}(t) = \Gamma_{iy}\mathrm{Proj}\{-\tilde{y}_i + k_y(\hat{\upsilon}_{iyf}(t) - \hat{\upsilon}_{iy}(t))\}, \\ \dot{\hat{\upsilon}}_{ixf}(t) = \Gamma_{ixf}\mathrm{Proj}\{\hat{\upsilon}_{ix}(t) - \hat{\upsilon}_{ixf}(t)\}, \\ \dot{\hat{\upsilon}}_{iyf}(t) = \Gamma_{iyf}\mathrm{Proj}\{\hat{\upsilon}_{iy}(t) - \hat{\upsilon}_{iyf}(t)\}. \end{cases} \tag{71}$$

The resulting closed-loop network system can be described by

$$\begin{cases} \dot{z}_{i1} = -K_{i1}s_i + R_iz_{2i} - \tilde{V}_{ic}(t), \\ M_i\dot{z}_{i2} = -K_{i2}z_{i2} - R_i^Ts_i + \tilde{W}_i^T(t)\varphi_i(\chi_i) - \varepsilon_i, \\ \dot{\tilde{x}}_i = -\kappa_{i1}\tilde{x}_i + \tilde{\upsilon}_{ix}, \\ \dot{\tilde{y}}_i = -\kappa_{i2}\tilde{y}_i + \tilde{\upsilon}_{iy}. \end{cases} \tag{72}$$

where $\tilde{V}_{ic}(t) = \hat{V}_{ic}(t) - V_{ic}(t)$.

It is the position to state the third result of this paper.

**Theorem 3** Consider a networked system consisting of $N$ MSVs governed by the dynamics (5, 6) with Assumptions 1 and 2 satisfied. Select the control laws (70) with the adaptive laws (71). Then, all signals in the closed-loop system are UUB, and the formation pattern control errors $\eta_i - \eta_j - \mathcal{P}_{ij}$ satisfy (8) for some constant $\delta_1$, provided that

$$\begin{aligned} &\lambda_{\min}(K_1) > 1/2, \lambda_{\min}(K_2) > 1/2, \\ &\lambda_{\min}(\kappa_1) > 1/2, \lambda_{\min}(\kappa_2) > 1/2. \end{aligned} \tag{73}$$

*Proof* Take the following Lyapunov function candidate

$$\mathcal{V}_3 = \mathcal{V}_1 + \mathcal{V}_o, \tag{74}$$

whose time derivative along (72) and (71) can be put into

$$\begin{aligned} \dot{\mathcal{V}}_3 = &-s^TK_1s - z_2^TK_2z_2 - s^T\tilde{V}_c - z_2^T\varepsilon - \mathrm{tr}[(\tilde{W}^T\Gamma_W^{-1} \\ &+ k_W\tilde{W}_f^T\Gamma_f^{-1})\dot{W}] - \tilde{x}^T\kappa_1\tilde{x} - \tilde{y}^T\kappa_2\tilde{y} - (\tilde{\upsilon}_x^T\Gamma_x^{-1} \\ &+ k_x\tilde{\upsilon}_{fx}^T\Gamma_{xf}^{-1})\dot{v}_x - (\tilde{\upsilon}_y^T\Gamma_y^{-1} + k_y\tilde{\upsilon}_{fy}^T\Gamma_{yf}^{-1})\dot{v}_y. \end{aligned} \tag{75}$$

Using Young's inequality, it is easy to verify that

$$\begin{aligned} \dot{\mathcal{V}}_3 \leq &-[\lambda_{\min}(K_1) - 1/2]\|s\|^2 - [\lambda_{\min}(K_2) - 1/2]\|z_2\|^2 \\ &- [\lambda_{\min}(\kappa_1) - 1/2]\|\tilde{x}\|^2 - [\lambda_{\min}(\kappa_2) - 1/2]\|\tilde{y}\|^2 + \epsilon_s, \end{aligned}$$

with $\epsilon_s = \epsilon + \epsilon_o$.

Using (73) and noting that either $\|s\| > \sqrt{\epsilon_s/[\lambda_{\min}(K_1) - 1/2]}$, or $\|z_2\| > \sqrt{\epsilon_s/[\lambda_{\min}(K_2) - 1/2]}$, or $\|\tilde{x}\| > \sqrt{\epsilon_s/[\lambda_{\min}(\kappa_1) - 1/2]}$, or $\|\tilde{y}\| > \sqrt{\epsilon_s/[\lambda_{\min}(\kappa_2) - 1/2]}$ renders $\dot{\mathcal{V}}_3 < 0$, it follows that $s$, $z_2$, $\tilde{x}$, $\tilde{y}$ are UUB. Using inequality (37), it follows that $\|z_1 - \mathbf{1}\otimes\mathrm{Ave}(z_1)\| \leq \sqrt{\frac{2\lambda_{\max}(P)\epsilon_s}{\lambda_2(L)[\lambda_{\min}(K_1) - 1/2]}}$. Similarly, we can derive that (8) is satisfied with $\delta_1$ taken as

$$\delta_1 = 2\sqrt{\frac{2\lambda_{\max}(P)\epsilon_s}{\lambda_2(L)[\lambda_{\min}(K_1) - 1/2]}}, \tag{76}$$

which can be reduced as desired. This completes the proof. □

### 4.3 Leader-follower formation pattern control

In this case, taking the time derivative of $q_{i1}$ yields

$$\dot{q}_{i1} = R_i\alpha_{i2} + R_iq_{i2} + V_{ic}(t), \tag{77}$$

Then, a distributed kinematic control law $\alpha_{i2}$ is proposed as follows

$$\alpha_{i2} = -K_{i1}R_i^T\zeta_i - R_i^T\hat{V}_{ic}(t), \tag{78}$$

Similarly, the leader-follower formation controller under time-varying ocean currents is summarized as follows.

Control laws:

$$\begin{cases} \tau_i = \hat{W}_i^T(t)\varphi_i(\chi_i) - K_{i2}q_{i2} - R_i^T\zeta_i, \\ \alpha_{i2} = -K_{i1}R_i^T\zeta_i - R_i^T\hat{V}_{ic}(t), \\ \dot{\tilde{x}}_i = u_i\cos(\psi_i) + v_i\sin(\psi_i) + \hat{\upsilon}_{ix}(t) - \kappa_{i1}\tilde{x}_i, \\ \dot{\tilde{y}}_i = u_i\sin(\psi_i) + v_i\cos(\psi_i) + \hat{\upsilon}_{iy}(t) - \kappa_{i2}\tilde{y}_i, \end{cases} \tag{79}$$

Adaptive laws:

$$\begin{cases} \dot{\hat{W}}_i(t) = \Gamma_{iW}\mathrm{Proj}\{-\varphi_i(\chi_i)q_{i2}^T + k_W[\hat{W}_{if}(t) - \hat{W}_i(t)]\}, \\ \dot{\hat{W}}_{if}(t) = \Gamma_{if}\mathrm{Proj}\{\hat{W}_i(t) - \hat{W}_{if}(t)\}, \\ \dot{\hat{\upsilon}}_{ix}(t) = \Gamma_{ix}\mathrm{Proj}\{-\tilde{x}_i + k_x(\hat{\upsilon}_{ixf}(t) - \hat{\upsilon}_{ix}(t))\}, \\ \dot{\hat{\upsilon}}_{iy}(t) = \Gamma_{iy}\mathrm{Proj}\{-\tilde{y}_i + k_y(\hat{\upsilon}_{iyf}(t) - \hat{\upsilon}_{iy}(t))\}, \\ \dot{\hat{\upsilon}}_{ixf}(t) = \Gamma_{ixf}\mathrm{Proj}\{\hat{\upsilon}_{ix}(t) - \hat{\upsilon}_{ixf}(t)\}, \\ \dot{\hat{\upsilon}}_{iyf}(t) = \Gamma_{iyf}\mathrm{Proj}\{\hat{\upsilon}_{iy}(t) - \hat{\upsilon}_{iyf}(t)\}. \end{cases} \tag{80}$$

The resulting closed-loop network system can be described by

$$\begin{cases} \dot{q}_{i1} = -K_{i1}\zeta_i + R_iq_{2i} - \tilde{V}_{ic}(t), \\ M_i\dot{q}_{i2} = -K_{i2}q_{i2} - R_i^T\zeta_i + \tilde{W}_i^T(t)\varphi_i(\chi_i) - \varepsilon_i, \\ \dot{\tilde{x}}_i = -\kappa_{i1}\tilde{x}_i + \tilde{\upsilon}_{ix}, \\ \dot{\tilde{y}}_i = -\kappa_{i2}\tilde{y}_i + \tilde{\upsilon}_{iy}. \end{cases} \tag{81}$$

The following theorem states the fourth result of this paper.

**Theorem 4** Consider a networked system consisting of $N$ MSVs governed by the dynamics in (5, 6) with Assumptions 1–2 satisfied, and at least, one MSV has access to $\eta_r$. Select the control laws (79) with the adaptive laws (80). Then, all the signals in the closed-loop system are UUB, and the leader-follower formation pattern control errors satisfy (9) for some constant $\delta_2$ and the formation center arrives at $\eta_r$ with bounded errors $\delta_3$ given by (10), provided that

$$\begin{aligned} &\lambda_{\min}(K_1) > 1/2, \lambda_{\min}(K_2) > 1/2 \\ &\lambda_{\min}(\kappa_1) > 1/2, \lambda_{\min}(\kappa_2) > 1/2. \end{aligned} \tag{82}$$

*Proof* Following the same steps as in proving the Theorems 2 and 3, the stability of multi-vehicle systems can be established by taking the Lyapunov candidate $\mathcal{V}_4 = \mathcal{V}_2 + \mathcal{V}_o$. The proof details are omitted here for brief.

## 5 An example

Consider a networked system that consists of five vehicles whose model parameters can be found in Table 1 [36]. Let the information topology among the five vehicles be given by Fig. 2. We first consider the leader-follower formation pattern control case without ocean currents. Next, we consider the leader-follower formation pattern control under time-varying ocean currents.

### 5.1 Case 1: leader-follower formation pattern control

In this case, the pattern controller given in Theorem 2 is applied. The control parameters are selected as follows $K_{i1} = \mathrm{diag}\{0.2, 0.2, 0.2\}, K_{i2} = \mathrm{diag}\{75, 22, 68.4\}$, $\Gamma_{iW} = 1000$, $\Gamma_{if} = 2$, $k_W = 0.1$. The NN activation function is chosen as $\frac{1}{1+e^{2x}}$. The desired formation pattern is set to $\mathcal{P}_1 = [-0.7, 0, 0]^{\mathrm{T}}$, $\mathcal{P}_2 = [-0.7\cos(72^\circ), 0.7\sin(72^\circ), 0]^{\mathrm{T}}$, $\mathcal{P}_3 = [-0.7\cos(72^\circ), -0.7\sin(72^\circ), 0]^{\mathrm{T}}$, $\mathcal{P}_4 = [0.7\cos(36^\circ), 0.7\sin(36^\circ), 0]^{\mathrm{T}}$, $\mathcal{P}_5 = [0.7\cos(36^\circ), -0.7\sin(36^\circ), 0]^{\mathrm{T}}$.

Let the MSV 2 have access to a series of way-points $\eta_r = \{(-1, -1, 0)^{\mathrm{T}}, (0, 0, 45^\circ)^{\mathrm{T}}, (1, 1, 45^\circ)^{\mathrm{T}}, (2, 1, 0)^{\mathrm{T}}, (3, 1, 0)^{\mathrm{T}}, (4, 1, 0)^{\mathrm{T}}, (5, 0, -45^\circ)^{\mathrm{T}}, (6, -1, -45^\circ)^{\mathrm{T}}\}$. Simulation results are provided in Figs. 3, 4, 5 and 6. Figure 3 shows the entire formation geometries of the five MSVs with information-exchange given by Fig. 2. It can be observed that a star formation is well maintained. Figure 4 plots the uncertainty and outputs of NNs associated with the MSV 1. It can be seen that only the low frequency content of the uncertainty can be learned by NNs. Figure 5 shows the approximation profile under different frequencies of disturbances. It reveals that the learning errors do not increase as the frequency of uncertainty increase. However, the high frequency content will be filtered by the developed adaptive laws. Figure 6 shows the boundedness and smoothness of control signals.

**Table 1** Model parameters

| Parameters | Value |
|---|---|
| $m_{i11}$ | 25.8 |
| $m_{i22}$ | 33.8 |
| $m_{i23} = m_{i32}$ | 1.0115 |
| $c_{i13} = -m_{i31}$ | −33.8v–1.0115r |
| $c_{i23} = -m_{i32}$ | $25.8u$ |
| $d_{i11}$ | $0.72 + 1.33\lvert u\rvert + 5.87u^2$ |
| $d_{i22}$ | $0.8896 + 36.5\lvert v\rvert + 0.805\lvert r\rvert$ |
| $d_{i23}$ | $7.25 + 0.845\lvert v\rvert + 3.45\lvert r\rvert$ |
| $d_{i32}$ | $0.0313 + 3.96\lvert v\rvert + 0.130\lvert r\rvert$ |
| $d_{i33}$ | $1.90 - 0.080\lvert v\rvert + 0.75\lvert r\rvert$ |
| $g_{iu}$ | $0.0279uv^2 + 0.0342v^2r$ |
| $g_{iv}$ | $0.0912u^2v + 0.0232ur$ |
| $g_{ir}$ | $0.0156ur^2 + 0.0278urv^3$ |

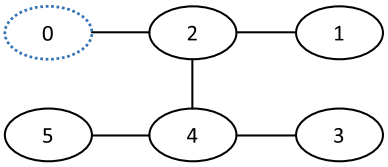


**Fig. 2** Communication topology

### 5.2 Case 2: leader-follower formation pattern control under time-varying ocean currents

We start with introducing an ocean current model for simulation. The model for ocean currents in two dimensions is characterized by its velocity $V_{oc}(t)$ and earth-fixed direction $\beta_c(t)$. In the earth-fixed frame, the current model is described by

$$\upsilon_x(t) = V_{oc}(t)\cos\beta_c(t);\ \upsilon_y(t) = V_{oc}(t)\sin\beta_c(t). \tag{83}$$

For simulations, the ocean current speed $V_{oc}(t)$ and direction $\beta_c(t)$ can be generated by using first-order Gauss-Markov processes

$$\dot{V}_{oc}(t) + \varrho_1 V_{oc}(t) = w_1(t);\ \dot{\beta}_c(t) + \varrho_2\beta_c(t) = w_2(t); \tag{84}$$

where $w_i\ (i = 1, 2)$ are zero-mean Gaussian white noise processes and $\varrho_i\ (i = 1, 2)$ are constants. A saturating element is used in the integration process to limit the current speed to $V_{\min} \le V_{oc}(t) \le V_{\max}$ with $V_{\min} = 0.18$ and $V_{\max} = 0.22$. The direction of the current is fixed by specifying a constant value for $\beta_c = 45°$. As for the model introduction of ocean currents, the readers are referred to [41]. In this case, the pattern controller given in Theorem 4 is applied the group. The control parameters are selected as the same as above; others are chosen as $\Gamma_{ix} = \Gamma_{iy} = 100, \Gamma_{ifx} = \Gamma_{ify} = 2, k_x = k_y = 0.1$. The desired formation center is set to $\eta_r = \{(2, -1, 0°)^{\mathrm{T}}, (5, 1, 45°)^{\mathrm{T}}\}$. Simulation results are shown in Figs. 7, 8, 9 and 10. Figure 7 shows that the formation pattern cannot be stabilized due to the time-varying ocean currents. By contrast, Fig. 8 demonstrates the formation is well maintained by the proposed observer-based formation controller. Figure 9 verifies that the time-varying ocean currents can be identified accurately by the proposed observer. Figure 10 demonstrates the formation pattern transition from one to another under time-varying ocean currents.

## 6 Conclusions

This paper considered the coordinated formation pattern control of multiple marine surface vehicles in the presence of dynamical uncertainty and ocean disturbances induced by unknown wind, waves and ocean currents. Neural networks, adaptive filtering and backstepping techniques are employed to develop the distributed formation pattern

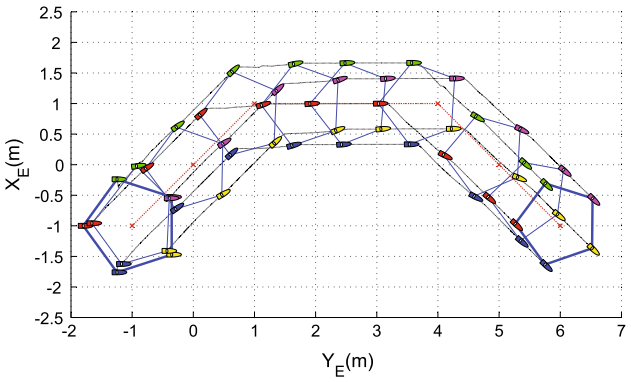


**Fig. 3** Formation trajectories

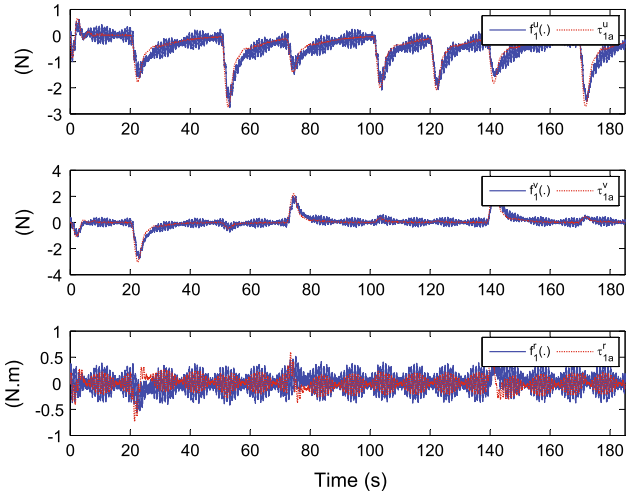


**Fig. 4** Approximation of NNs corresponding to MSV 1

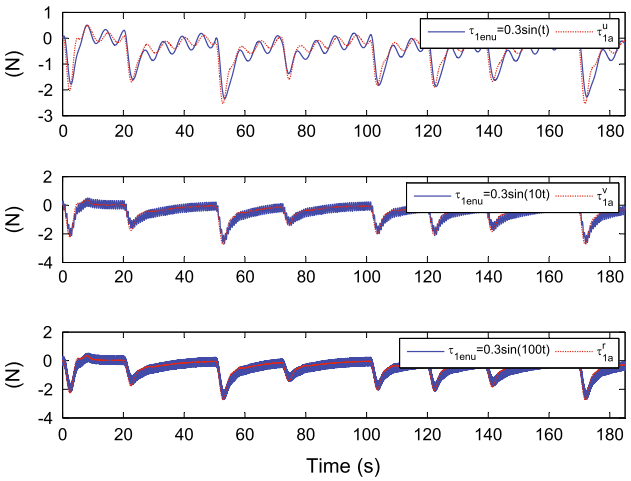


**Fig. 5** Approximation comparisons under different frequencies of disturbances

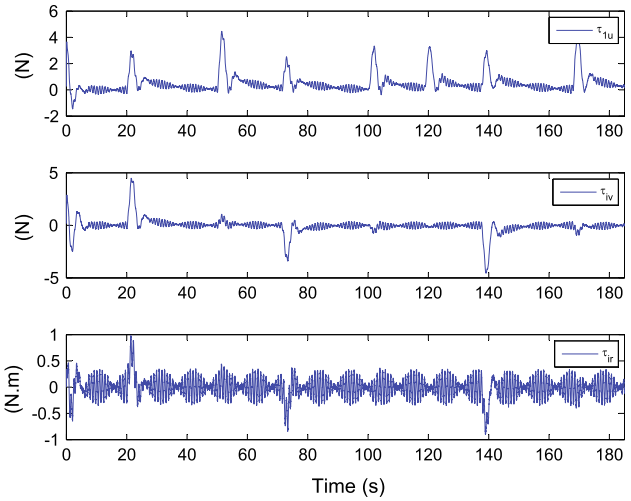


**Fig. 6** Control effort in each direction corresponding to MSV 1

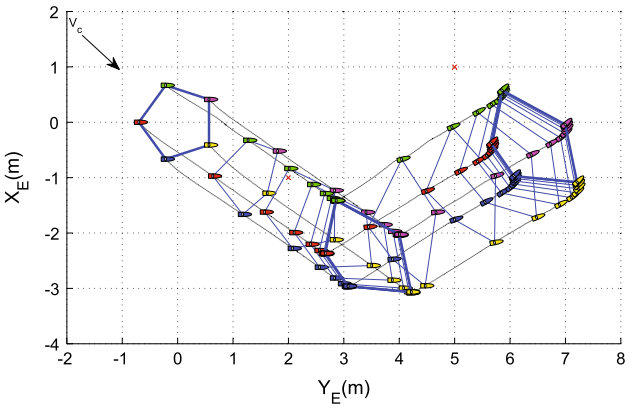


**Fig. 7** Formation trajectories without observer ($t = 120$ s)

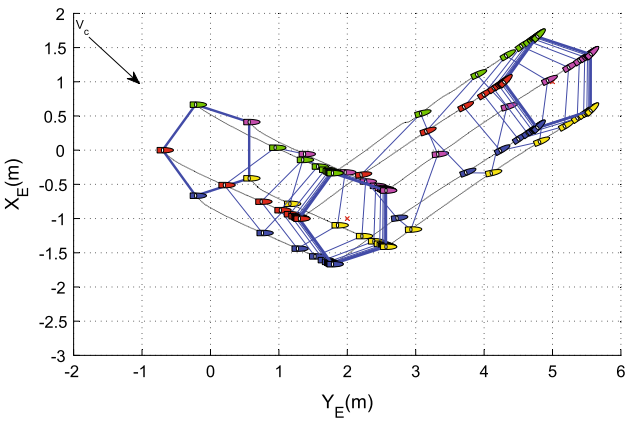


**Fig. 8** Formation trajectories with observer ($t = 120$ s)

controllers, under which a stationary formation can be reached for any undirected connected graphs. Lyapunov stability analysis demonstrates that all signals in the closed-loop systems are uniformly ultimately bounded. The main advantage lies in the fact that the proposed control scheme leads to adaptive formation pattern controllers with guaranteed low frequency control signals, which facilities the practical implementations under hazardous sea environment. Simulation results showed the efficacy of the proposed cooperative controllers. Future works include extensions to distributed formation pattern control in the presence of unmeasured velocities, input constraint, measurement noises and communication delays. So far, these problems have not been well addressed due to technical obstacles.

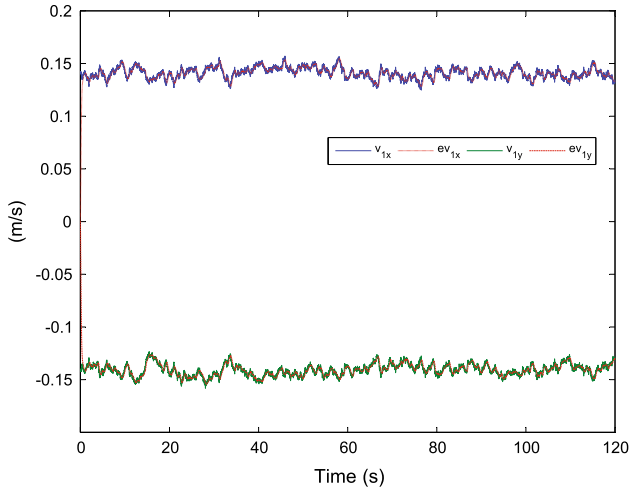


**Fig. 9** Estimation of ocean currents ($ev_{1x}$ denotes the estimate of $v_{1x}$; $ev_{1y}$ denotes the estimate of $v_{1y}$)

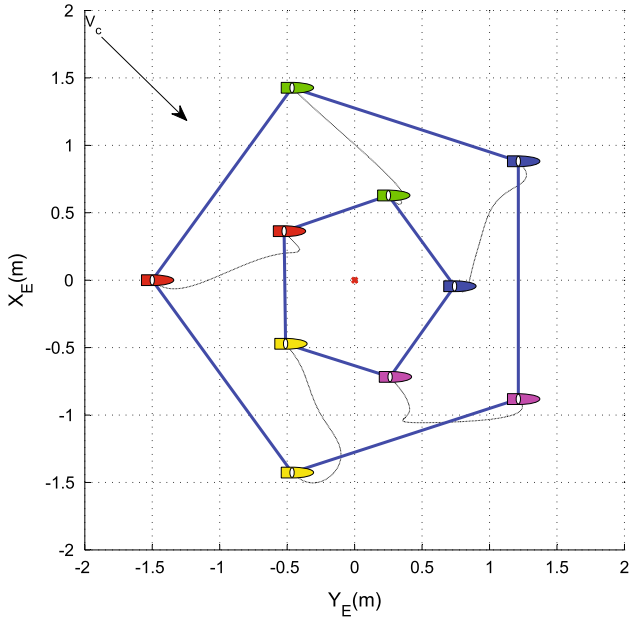


**Fig. 10** Formation transition

**Acknowledgments** This work was supported in part by the National Nature Science Foundation of China under Grants 51209026, 61273137 and 61074017, and in part by the Scientific Research Fund of Liaoning Provincial Education Department under Grant L2013202 and in part by the Fundamental Research Funds for the Central Universities 3132014047 and 3132014321. We also would like to thank Dr. Hongwei Zhang for discussing and revising this paper.

## References

1. Jadbabaie A, Lin J, Morse AS (2003) Coordination of groups of mobile autonomous agents using nearest neighbor rules. IEEE Trans Autom Control 48(6):988–1001
2. Fax JA, Murray RM (2004) Information flow and cooperative control of vehicle formations. IEEE Trans Autom Control 49(9):1465–1476
3. Skjetne R, Moi S, Fossen TI (2002) Nonlinear formation control of marine vessel. Decis Control 2:1699–1704
4. Arrichiello F, Chiaverini S, Fossen TI (2006) Formation control of underactuated surface vessels using the null-space-based behavioral control. International Conference on Intelligent Robots and Systems, pp 5942–5947
5. Peng ZH, Wang D, Hu XJ (2011) Robust adaptive formation control of underactuated autonomous surface vehicles with uncertain dynamics. IET Control Theory Appl 5(12):1378–1387
6. Cui RX, Ge SS, How BVE, Choo YS (2010) Leader-follower formation control of underactuated autonomous underwater vehicles. Ocean Eng 37(17–18):1491–1502
7. Peng ZH, Wang D, Chen ZY, Hu XJ, Lan WY (2013) Adaptive dynamic surface control for formations of autonomous surface vehicles with uncertain dynamics. IEEE Trans Control Syst Technol 21(2):513–520
8. Ihle I, Arcak FM, Fossen TI (2007) Passivity-based designs for synchronized path following. Automatica 43(9):1508–1518
9. Peng ZH, Wang D, Li TS, Wu ZL (2013) Leaderless and leader-follower cooperative control of multiple marine surface vehicles with unknown dynamics. Nonlinear Dyn 74(1–2):95–106
10. Hong YG, Hu JP, Gao LX (2006) Tracking control for multi-agent consensus with an active leader and variable topology. Automatica 42(7):1177–1182
11. Ren W (2007) Multi-vehicle consensus with a time-varying reference state. Syst Control Lett 56(7–8):474–483
12. Hou ZG, Cheng L, Tan M (2009) Decentralized robust adaptive control for the multiagent system consensus problem using neural networks. IEEE Trans Syst Man Cybern B 39(3):636–647
13. Das A, Lewis FL (2010) Distributed adaptive control for synchronization of unknown nonlinear networked systems. Automatica 46(12):2014–2021
14. Hu GQ (2012) Robust consensus tracking of a class of second-order multi-agent dynamic systems. Syst Control Lett 61(1):134–142
15. Das A, Lewis FL (2011) Cooperative adaptive control for synchronization of second-order system with unknown nonlinearities. Int J Robust Nonlinear Control 21(13):1509–1524
16. Chen WS, Li XB, Jiao LC (2013) Quantized consensus of second-order continuous-time multi-agent systems with a directed topology via sampled data. Automatica 49(7):2236–2242
17. Chen WS, Li XB (2014) Observer-based consensus of second-order multi-agent systems with fixed and stochastically switching topology via sampled data. Int J Robust Nonlinear Control 24(3):567–584
18. Zhang HW, Lewis FL (2012) Adaptive cooperative tracking control of higher-order nonlinear systems with unknown dynamics. Automatica 48(7):1432–1439
19. Wang XL, Hong YG, Huang J, Jiang ZP (2010) A distributed control approach to a robust output regulation problem for multi-agent linear systems. IEEE Trans Autom Control 55(12):2891–2895
20. Hong YG, Wang XL, Jiang ZP (2013) Distributed output regulation of leader-follower multi-agent systems. Int J Robust Nonlinear Control 23(1):48–66
21. Li ZK, Duan ZS, Chen GR, Huang L (2010) Consensus of multiagent systems and synchronization of complex networks: a unified viewpoint. IEEE Trans Circuit Syst 57(1):213–224
22. Zhang HW, Lewis FL, Das A (2011) Optimal design for synchronization of cooperative systems: state feedback, observer and output feedback. IEEE Trans Autom Control 56(8):1948–1952
23. Wen GH, Duan ZS, Chen GR, Yu WW (2014) Consensus tracking of multi-agent systems with lipschitz-type node dynamics and switching topologies. IEEE Trans Circuits Syst I: Regul Pap 61(4):499–511
24. Zhang HW, Lewis FL, Qu ZH (2012) Lyapunov, adaptive, and optimal design techniques for cooperative systems on directed communication graphs. IEEE Trans Ind Electron 59(7):3026–3041
25. Fossen TI (2002) Marine control system. guidance, navigation and control of ships, rigs and underwater vehicles, Trondheim, Norway, Marine Cybernetics
26. Do KD, Pan J (2006) Global robust adaptive path following of underactuated ships. Automatica 42(10):1713–1722
27. Li JH, Lee PM, Jun BH, Lim YK (2008) Point-to-point navigation of underactuated ships. Automatica 44(12):3201–3205
28. Tee KP, Ge SS (2006) Control of fully actuated ocean surface vessels using a class of feedforward approximators. IEEE Trans Control Syst Technol 14(4):750–756
29. Chen M, Ge SS, How BVE, Choo YS (2013) Robust adaptive position mooring control for marine vessels. IEEE Trans Control Syst Technol 21(2):395–409
30. How BVE, Ge SS, Choo YS (2013) Dynamic load positioning for subsea installation via adaptive neural control. IEEE J Ocean Eng 35(2):366–375
31. Dai SL, Wang C, Luo F (2012) Identification and learning control of ocean surface ship using neural networks. IEEE Trans Ind Inform 8(4):801–810
32. Chen M, Ge SS, Choo YS (2009) Neural network tracking control of ocean surface vessels with input saturation. International Conference on Automation and Logistics, pp 85–89
33. Yucelen T, Haddad WM (2013) Low-frequency learning and fast adaptation in model reference adaptive control. IEEE Trans Autom Control 58(4):1080–1085
34. Aguiar AP, Pascoal AM (2007) Dynamic positioning and way-point tracking of underactuated AUVs in the presence of ocean currents. Int J Control 80(7):1092–1108
35. Almeida J, Silvestre C, Pascoal AM (2010) Cooperative control of multiple surface vessels in the presence of ocean currents and parametric model uncertainty. Int J Robust Nonlinear Control 20(14):1549–1565
36. Skjetne R, Fossen TI, Kokotovic PV (2005) Adaptive maneuvering, with experiments, for a model ship in a marine control laboratory. Automatica 41(2):289–298
37. Ceragiolia F, Persisb CD, Frascaa P (2011) Discontinuities and hysteresis in quantized average consensus. Automatica 47(9):1916–1928
38. Lavretsky E, Gibson TE (2012) Projection operator in adaptive systems. arXiv:1112.4232v5
39. Krstić M, Kanellakopoulos I, Kokotovic P (1995) Nonlinear and adaptive control design. Wiley, New York
40. Khalil HK (2002) Nonlinear systems. Prentice Hall
41. Fossen TI (2012) How to incorporate wind, waves and ocean currents in the marine craft equations of motion. Proc IFAC Conf Manoeuvring Control Mar Craft 9(1):126–131